Spectroscopic Studies of an Electron-Beam-Produced Plasma

By

Takashi FUJIMOTO*, Yuji NISHIMURA* and Atsumu HIRABAYASHI*

(Received September 29, 1983)

Abstract

An electron beam operating in medium-pressure gases has been constructed, and its operating characteristics investigated. Helium, neon and argon have been excited by the electron beam, and it has been found that for lower pressures, less than 1 torr in the case of helium, accelerated electrons directly excite the ionic excited level. The population densities in the neutral series levels have been observed up to $n=15$, and have been found to be roughly proportional to n^{-4}. A possible explanation is proposed that is based on a direct excitation from the ground state and a depopulation by l-changing collisions.

§1. Introduction

Fusayama and Dote[1] have proposed an electron-beam concept that operates under medium-pressure gas conditions. This idea is based on the scaling of Paschen's law: the breakdown voltage is a function of pD, the product of the pressure and the distance between two electrodes. If the distance D is made sufficiently small, we may increase the pressure p to a certain value without inducing a breakdown between the electrodes. The apparatus consists of a plasma cathode part and an accelerating electrode. The anode of the plasma cathode discharge and the accelerating electrode are made of mesh and are closely spaced each other. When we apply high voltages to the latter electrode, we extract and accelerate electrons from the plasma cathode discharge. Thus, we obtain an electron beam without causing a breakdown.

Unlike the standard electron beam this apparatus produces atomic ions in ambient gases, and this method should be very useful for studying collision processes of ions with neutral atoms. We have constructed this apparatus and have made a preliminary experiment. The following describes the results.

§2. Experiment

Figure 1 shows the block diagram of the plasma-cathode electron-beam appara-

* Department of Engineering Science

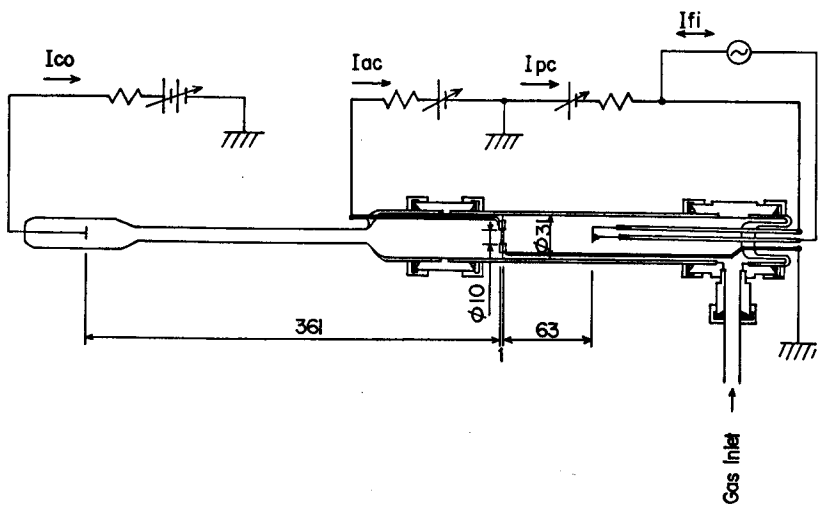

Fig. 1. Schematic diagram of the plasma-cathode electron-beam apparatus. The anode and the accelerating electrode are separated by a hollow glass wall.

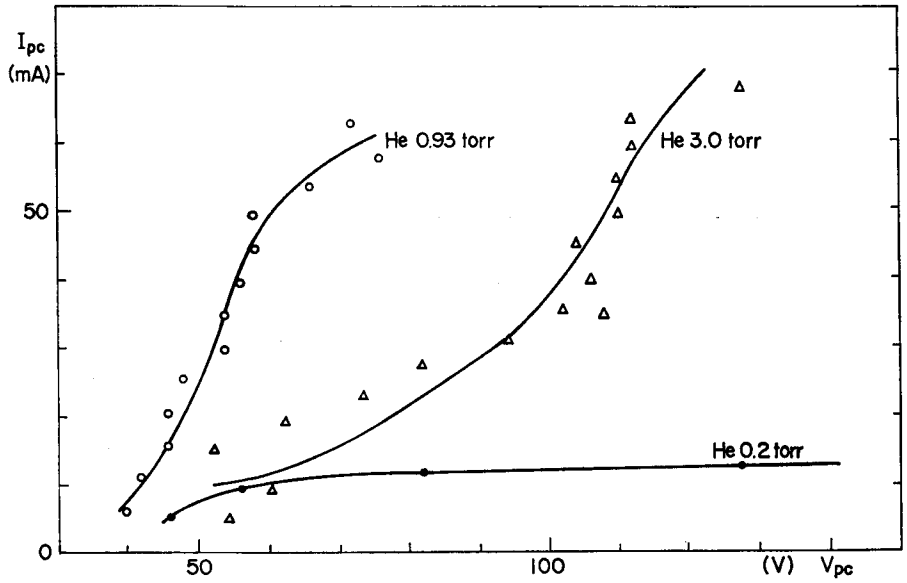

Fig. 2. The V_{pc}—I_{pc} curve for the plasma cathode discharge in helium.

tus. The plasma cathode section consists of a helically-wound cone-shaped tungsten filament (0.5 mm diameter wire) hot cathode and a molybdenum mesh (100 mesh/inch, 0.05 mm diameter wire) anode. An ac current of 14 A was applied to the filament, and its temperature was estimated from the *V-I* characteristics to be about 2400°C. The distance between the hot cathode and the grounded anode was 63 mm. In order to avoid a parasitic discharge between the cathode and the

anode lead wire, a glass sleeve was applied to the latter. The V_{pc}-I_{pc} characteristic of the plasma-cathode discharge is shown in Fig. 2. (V_{pc} and I_{pc} are, respectively, the voltage and the current of the plasma-cathode discharge.) A maximum current of 60 mA is achieved for a moderate applied voltage of 70 V for the 1 torr pressure.

Electrons in the plasma-cathode discharge are extracted through the mesh anode by a field applied with an accelerating electrode that is made of a molybdenum mesh, and placed 1 mm from the anode. (Fig. 1) Both electrodes have active diameters of 10 mm, and they are separated by a hollow glass ring insulator. A collecting electrode is placed 36 cm further downstream.

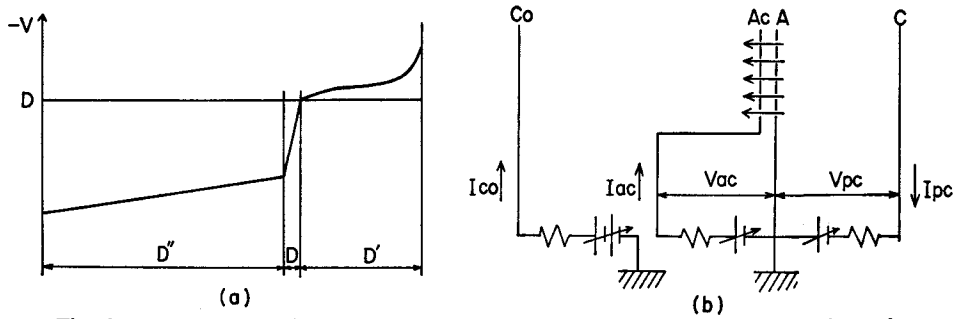

Fig. 3. (a) The potential distribution over the plasma cathode, accelerating electrode and collecting electrode. (b) The electrical connections and the applied voltages among the electrodes.

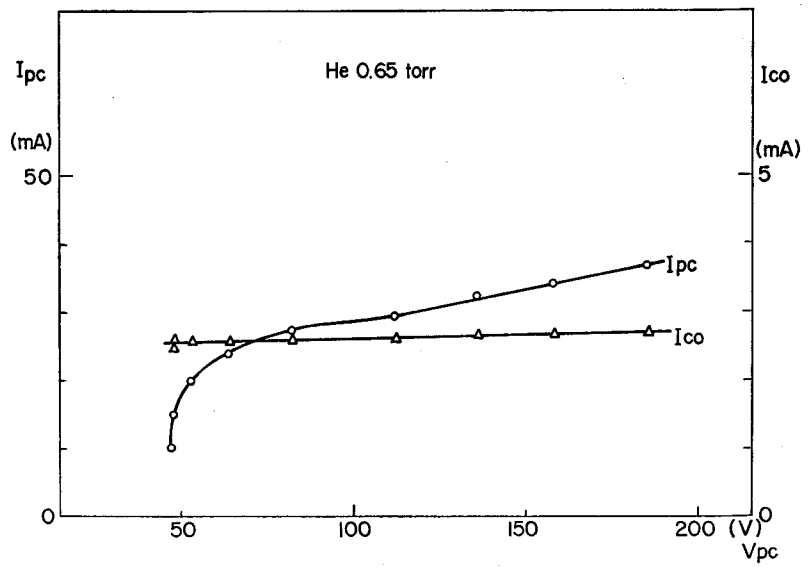

Fig. 4. The V_{pc}-dependences of the plasma-cathode current (I_{pc}) and of the collecting-electrode (I_{co}) current. The latter has no obvious correlation to the former.

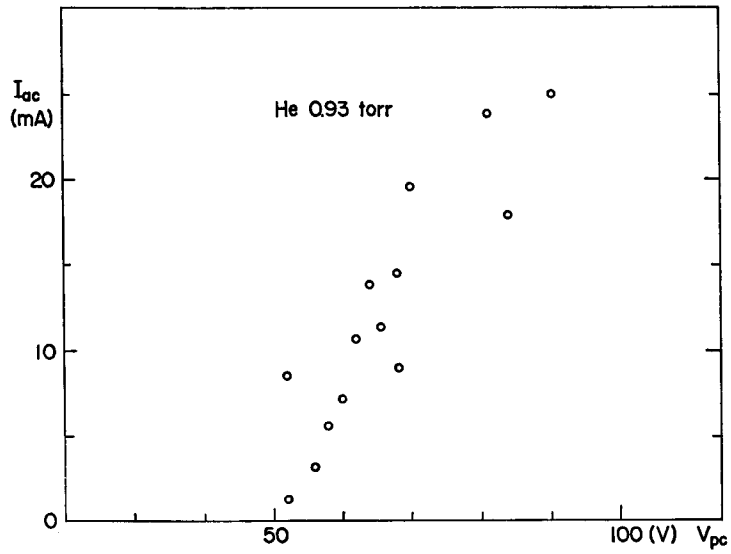

Fig. 5. The V_{pc}-dependences of the accelerating-electrode current.

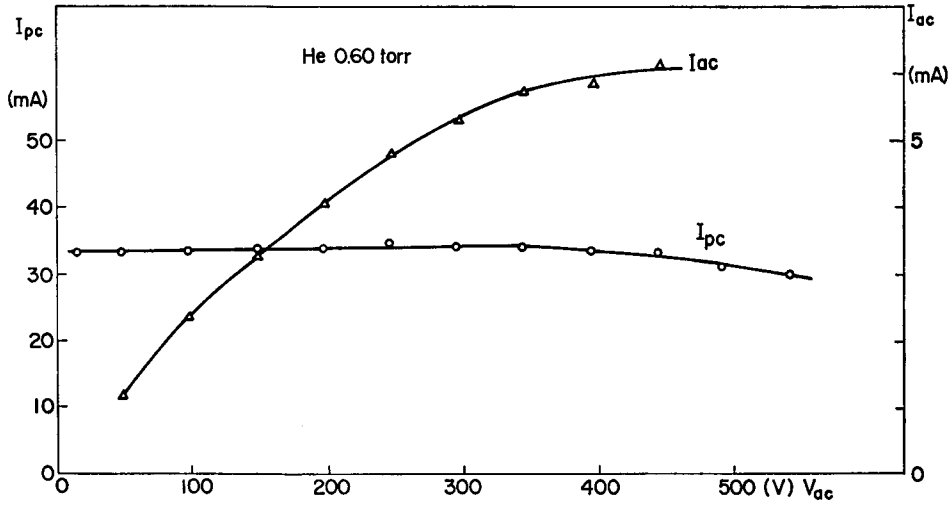

Fig. 6. The V_{ac}-dependences of the plasma-cathode current and of the accelerating-electrode current. An increase in the electron-beam current with an increase in V_{ac} is inferred.

Figure 3 shows the schematics of the electrical connection of the electrodes along with a potential curve for electrons over the discharge tube. Figures 4 ~6 give examples of various *V-I* characteristics for discharge conditions under which a discharge takes place between the accelerating electrode and the collecting electrode. To maintain the discharge, a voltage of 1.5 kV was applied to the collecting electrode

through a 130 kΩ resistor. Just downstream from the accelerating electrode, a greenish luminous plasma column was formed that was apparently excited by the electron beam. Further downstream, the color changed to pink, indicating that the plasma is essentially a normal positive column. Figures 4 and 5 show the V_{pc}-dependences of various currents. These data are taken for a constant accelerating voltage $V_{ac}=400$ V. The plasma-cathode current I_{pc} in Fig. 4 is, being consistent with Fig. 2, strongly dependent on V_{pc}, especially for small V_{pc}. Since the electron density in the plasma-cathode region should be roughly proportional to the discharge current I_{pc}, the extracted electron-beam current is expected to be proportional to I_{pc}. The collector current, I_{co}, on the other hand, is almost independent of V_{pc} or I_{pc}. This fact suggests that I_{co} does not have strong correlation with the electron-beam current. In Fig. 5, it is seen that the accelerating current I_{ac} is strongly dependent on V_{pc} or the electron density, roughly consistent with Fig. 2 for the same pressure. Thus, it is suggested that I_{ac} consists of two parts: the first is the directly absorbed current at the mesh, and the second is the extracted current. Its electrons somehow return to the accelerating electrode, and both are proportional to n_e. Figure 6 shows that the plasma-cathode discharge is almost independent of V_{ac}, and that the electron beam current increases with an increase in the accelerating voltage. A factor 2 increase may be suggested for an increase in V_{ac} from 150 V to 500 V.

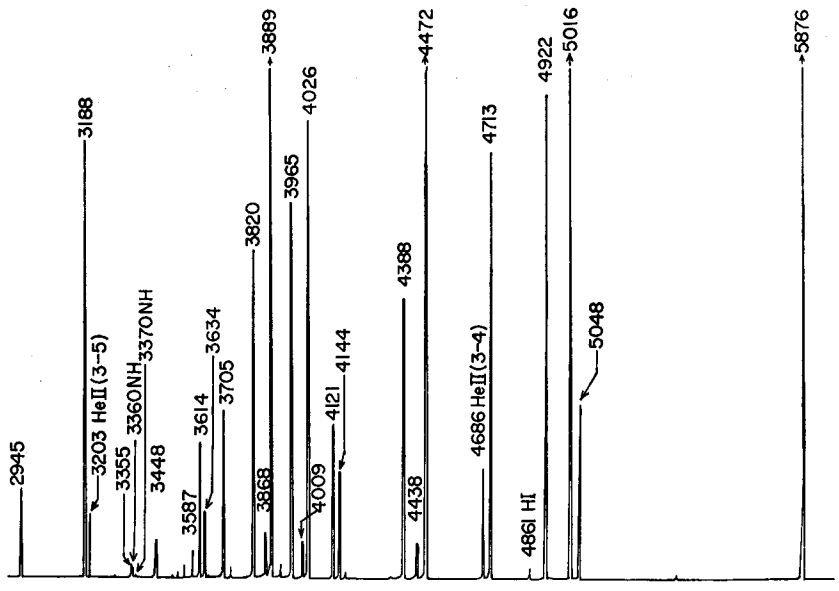

Fig. 7. The spectrum of the helium plasma produced by the electron-beam, 5 mm downstream from the accelerating electrode. $p=1.0$ torr.

As suggested in §1, a breakdown occurs when V_{ac} exceeds the breakdown voltage given by Paschen's law. Under our experimental condition, a breakdown did not occur up to $V_{ac}=500$ V for $p\lesssim 3$ torr. For 8 torr, a breakdown occurred at about 450 V.

§3. Spectroscopic Observation

3.1. Helium

Emission radiations from a plasma 5 mm downstream from the accelerating electrode were observed with a monochromator ($f/5$, focal length 25 cm and linear reciprocal dispersion 34 A/mm) and a photomultiplier (HTV R928). The entrance and exit slits had widths of 50 μm. Figure 7 shows an example of the spectra for helium, where the pressure was 1.0 torr, $I_{pc}=50$ mA and $V_{ac}=300$ V. It is noted that ionized helium lines of 4686 A (3—4) and 3203 A (3—5) are observed among strong neutral lines. At higher pressures the 4650 A band of He_2 is observed, and

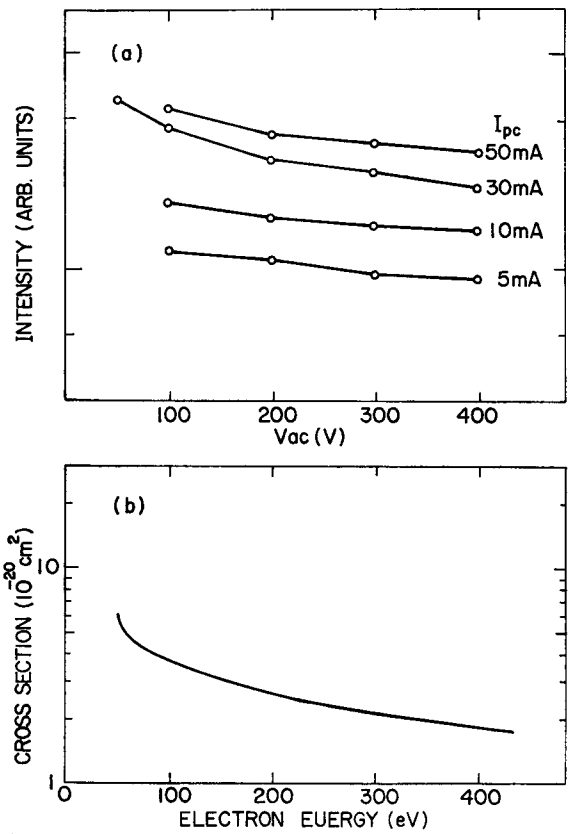

Fig. 8. (a) The V_{ac}-dependence of the emission intensity of HeI 4438 A (2^1P-5^1S). $p=0.5$ torr. (b) The excitation cross section of He 5^1S.

at 6 torr, the bandhead at 4648.5 A becomes stronger than the 4686 A line. Figures 8 and 9 show the dependence of the line intensities on V_{ac} ($p=0.5$ torr). Figure 8(a) is for HeI 4438 A (2^1P—5^1S). This shows that the emission line intensity decreases with an increase in V_{ac}. Figure 8(b) shows the excitation cross section by electron collision: $He(1^1S)+e \rightarrow He(5^1S)+e$[2]. If we take into account the fact that the electron-beam current increases by a factor 2 for an increase in V_{ac}, the dependence of the emission intensity on V_{ac} is well interpreted from the direct excitation from the ground state by the electron beam which is assumed to have an energy close to V_{ac}. Figure 9 is the corresponding figure for the HeII 4686 A (3—4) line. The V_{ac}-dependence is also interpreted by the direct ionization-excitation mechanism: $He(1^1S)+e \rightarrow He^+(4)+2e$[3].

For higher pressures, e.g., at 1 torr, the V_{ac}-dependences of the emission intensities become different from Figs. 8 and 9. For the neutral line 4438 A, the

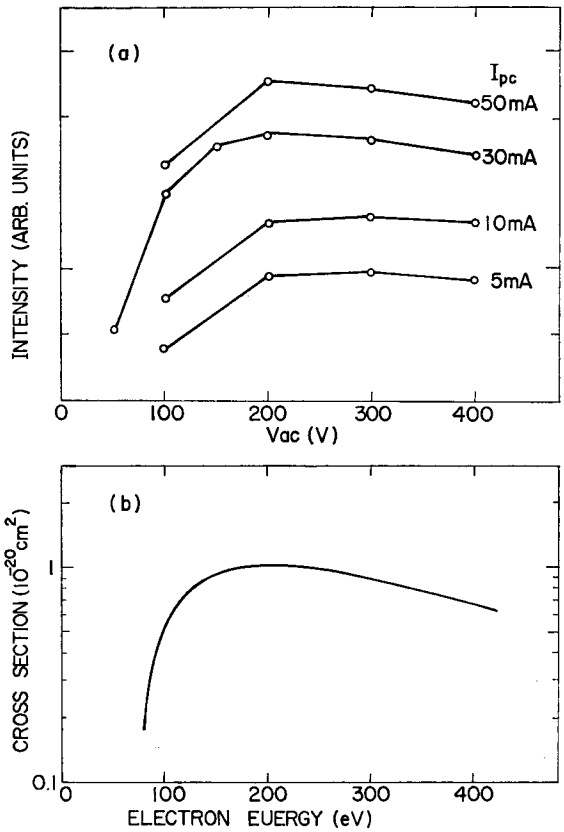

Fig. 9. (a) The V_{ac}-dependence of the emission intensity of HeII 4686 A (3—4). $p=0.5$ torr. (b) The ionization-excitation cross section of He^+ (4).

intensity increases instead of decreasing with an increasing V_{ac}. This may be interpreted by thermalization of the beam electron. The momentum-transfer collision cross section[4] for $He(1^1S)+e \rightarrow He(1^1S)+e$ is 3×10^{-17} cm^2 at the electron energy of 100 eV, and the mean free path for the collisions is about 1 cm at 1 torr. This gives the upper bound for the survival of the beam electron without appreciable deflection.

We observed several series lines of neutral helium. An example is seen in Fig. 7 for the 2^3P—n^3D and 2^1S—n^1P lines. The series limit is 3420 A for the former and 3120 A for the latter. We determined the relative population densities in the upper levels of the observed lines. The monochromator-photomultiplier system had been calibrated against a tungsten-ribbon standard lamp, and the absorption by the pyrex wall was also taken into account. Figure 10 shows an example: $p=1$ torr, $I_{pc}=50$ mA, $V_{ac}=300$ V and $I_{co}=3.1$ mA. Both series have a population

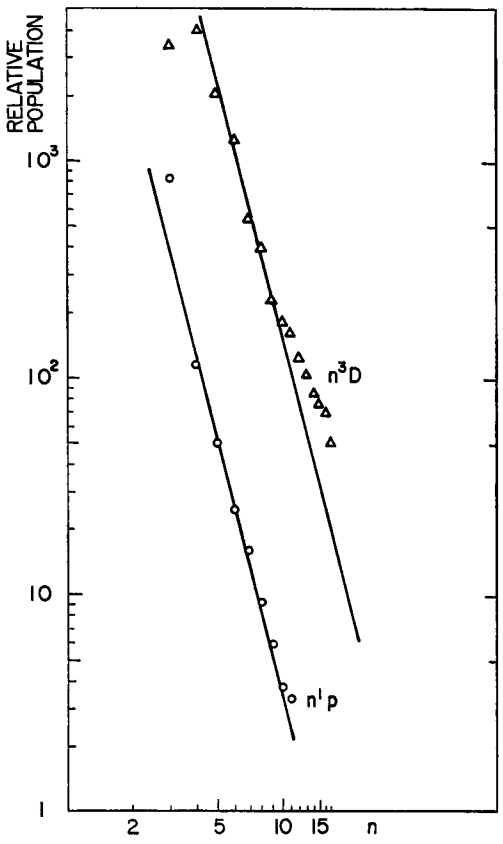

Fig. 10. The relative population-density distribution over the excited levels. $p=1$ torr. The lines show $\propto n^{-4}$.

density distribution approximately proportional to n^{-4}. We now consider a possible explanation.

1) **Corona equilibrium**
   direct excitation: proportional to n^{-3}
   radiative decay: proportional to n^{-3}
   population density: proportional to n^{0}
2) **Corona equilibrium (population is thermalized within the same n levels)**[5]
   radiative decay: proportional to $n^{-4.5}$
   population density: proportional to $n^{-0.5}$
3) **LTE (local thermodynamic equilibrium)**
   Since " the electron temperature " is very high the LTE population, if it existed[5], would be almost independent of n.
4) **Direct excitation and depopulation by l-changing collisions**
   depopulation: the population density in the low l levels observed is depleted to high l levels by the l-changing collisions by neutral helium atoms. The cross sections have been measured for " hydrogen like " levels for Rb(nf)+He by Hugon *et al.*[6]. It increases with n and has a maximum at $n\simeq 11$, then decreases. Thus, the resulting populations for small l levels may be close to $\propto n^{-4}$ for $n\lesssim 10$, $\propto n^{-3}$ for $n\simeq 11$, and $\propto n^{-2}$ for $n\geq 12$.
5) **The ladder-like excitation-ionization**[5]
   The stepwise electron collision excitation mechanism is established. Then, the population density is proportional to n^{-6}.

We find that among the above, only process 4) can explain the experimental result.

We made an observation of the plasma downstream in the small-bore tube section, but did not observe the helium ion lines. This suggested that the energetic electron beam component had disappeared before it reached there. The mean free path for an electron with an energy of 500 eV against momentum-transfer collisions is about 40 cm for $p=0.5$ torr. However, thermalizing collisions with other electrons and ions may cause the electron beam to diminish.

3.2 Neon and Argon

Figure 11 shows a part of the observed spectrum of neon excited by the electron beam. The pressure is 1 torr, $I_{ac}=27$ mA, $V_{ac}=200$ V and $I_{co}=4.9$ mA. The slit widths are 50 μm. Several strong ion lines are seen, the most prominent being the $3s$—$3p$ and $3p$—$3d$ transitions. In particular, the lines given below are anomalously strong in comparison with the intensities given in the standard table[7]: NeII 3324 A, 3344 A, 3378 A and 3393 A for $3s$—$3p$ transition array, NeII 3320 A for $3p$—$3d$ and 3569 A for $3s'$—$3p'$.

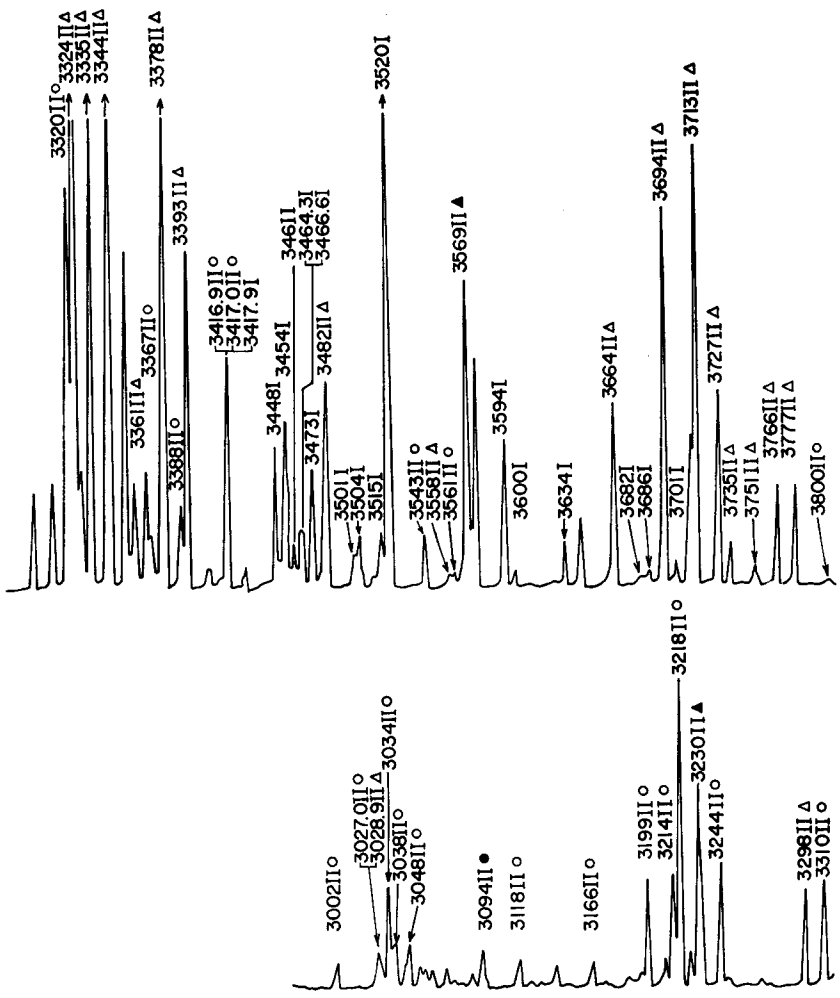

Fig. 11. The spectrum of the neon plasma produced by the electron beam, 5 mm downstream from the accelerating electrode. $p=1$ torr. I: NeI and II: NeII. ○: $3p-3d$, ●: $3p-4r$, △: $3s-3p$ and ▲: $3s'-3p'$.

For the argon spectrum, we identified more than 100 lines for ionized argon in the wavelength range of 2900 A through 5400 A. The most prominent are transitions in the $3p^44s$—$3p^44p$ transition array: 46 lines in total are observed, and some are very intense. Among them the $4s^4P$—$4p^4P°$ lines have lower intensities than the $4s^2P$—$4p^2P°$ lines. This is to be contrasted with the standard intensity ratio given in the table. Next prominent are the $4p$—$4d$, $4p$—$5s$ and $3d$—$4p$ transitions. A few transitions, namely $3d$—$4f$, $4s-5p$ and $4p$—$5d$, are observed.

In conclusion, the foregoing results show that the singly ionized excited levels are populated by direct excitation-ionization from the ground state neutral atom

by the beam electrons. These results also show that this apparatus is very promising for a study of collision processes involving these excited ions.

Note added in proof: Recently the depoulation cross sections from He(n^1P) ($4 \leq n \leq 13$) have been measured for collisions with He(1^1S). [W. R. Pendleton, Jr., M. Larsson and B. Mannfors: Phys. Rev. A 28, 3223 (1983).] The n-dependence is exactly the same as for Rb(nf). Thus the validity of the argument in (§3.1.4) is now confirmed.

References

1) T. Fusayama and T. Dote: (private communication).
2) H.R. Moustafa Moussa, F.J. de Heer and J. Schutten: Physica, **40**, 517 (1969).
3) J.F. Sutton and P.B. Kay: Phys. Rev. A, **9**, 697 (1974).
4) F.W. Byron and C.J. Joachain: FMO Report, No. **37**, 521 (1975).
5) T. Fujimoto: J. Phys. Soc. Japan: **47**, 265, 273 (1979).
6) M. Hugon, F. Gounand, P.R. Fournier and J. Berlande: J. Phys., B **12**, 2707 (1979).
7) A.N. Zaidel et al.: "Table of Spectral Lines" (Nauka, Moskow, 1969).